

D I P L O M A R B E I T

Localisation via ML Methods

Ausgeführt im Schuljahr 2019/20 von:

Algorithm	5AHIF
Ida Hönigmann	
System Engineering	5AHIF
Peter Kain	

Betreuer / Betreuerin:

MMag. Dr. Michael Stifter

Wiener Neustadt, am January 18, 2019/20

Abgabevermerk:

Übernommen von:

Eidestattliche Erklärung

Hiermit erkläre ich an Eides statt, dass ich die vorliegende Arbeit selbstständig und ohne fremde Hilfe verfasst und keine anderen als die im Literaturverzeichnis angegeben Quellen und Hilfsmittel verwendet habe. Insbesondere versichere ich, dass ich alle wörtlichen und sinngemäßen Übernahmen aus anderen Werken als solche kenntlich gemacht habe.

Wiener Neustadt am January 18, 2019/20

Verfasser / Verfasserinnen:

Ida HÖNIGMANN

Peter KAIN

Contents

Eidestattliche Erklärung	i
Acknowledgement	v
Kurzfassung	vi
Abstract	vii
1 Introduction	1
1.1 Goal	1
1.2 Motivation	2
1.3 Outlook and Perspective	2
1.4 Equipment	3
2 Study of Literature	5
2.1 Different Approaches to the Problem	5
2.2 Stereo Camera	5
2.2.1 Distortion	5
2.2.2 Image Rectification	6
2.2.3 Disparity Map	7
2.2.4 3D Point Cloud	8
2.3 LIDAR	8
2.4 Structure from Motion	8
2.5 Depth Maps from Structured Light	8
2.6 Human Depth Perception	9
2.6.1 Depth Sensation	10
3 Methodology	12
3.1 Challenges in the Use of Stereo Cameras	12
3.2 Generating Data	12
3.2.1 Blender	12
3.3 Image Preprocessing	14
3.4 Neural Network	16
3.4.1 Convolutional Neural Network	16

3.4.2	Loss Function	17
3.4.3	Activation Function	18
3.4.4	Initializer	19
3.4.5	Optimizer	20
3.4.6	Overfitting and Underfitting	21
3.5	Neural Network Implementations	23
3.6	TensorFlow	23
3.6.1	Computation graph	23
3.6.2	Alternatives to Tensorflow	25
4	ROS2	27
4.1	What is ROS?	27
4.1.1	Nodes	27
4.1.2	27
4.2	Why use ROS?	27
4.3	Comparing ROS and ROS2	27
5	Implementation	28
5.1	Generating test data	28
5.1.1	Generating the Render-Pairs	29
5.2	OpenCV	31
5.2.1	Greyscale	31
5.2.2	Resolution	33
5.2.3	Cropping	34
5.2.4	Saturated	34
5.2.5	Brightness	35
5.3	Neural Network	36
5.3.1	Setting up the Neural Network	36
5.3.2	Problems Encountered: Normalizing	36
5.3.3	Problems Encountered: Accuracy and Metrics	37
5.3.4	Problems Encountered: Number of Training Images	38
5.3.5	First Results	38
5.3.6	Modifications to the Neural Network	42
5.4	C++ Implementation	43
5.4.1	Structure	44
5.5	Technical difficulties	45
6	Experiment 1	46
6.1	Environment	46
6.2	Setup	46
6.3	Sequence of Events	46
6.4	Results	46
7	Lessons learned	47

8	Experiment 2	48
8.1	Environment	48
8.2	Setup	48
8.3	Materials	48
8.4	Sequence of Events	48
8.5	Results	48
9	Conclusion	49

Acknowledgement

The authors would like to thank ...

Kurzfassung

asdf

Abstract

asdf

Chapter 1

Introduction

Author: Ida Höningmann

Robots are getting more and more mobile. While a few years ago their usage was mostly limited to aid factory automation, robots have found widespread adoption in a multitude of industries, such as self driving cars and autonomous delivery drones. A challenge frequently encountered is navigating in unknown environments, which either requires the robot to sense specific characteristics of its surroundings or to communicate with some external system.

The problem of navigation has been looked at from many different angles. One popular approach in mobile robotics is to use the GPS, an external positioning system. In order to determine the position of a robot using the GPS, it has to establish communication with at least four satellites. The exact position of each satellite as well as the current time is broadcast by the satellites. By measuring the time needed for the signal to reach the robot, the position can be calculated up to three meters accurately.

However, in some cases positioning a robot using external positioning methods is not possible. In the case of the GPS this can be due to obstacles interfering with the radio signals send by the satellites, for example occurring inside a building. In comparison this work focuses on a system that can navigate in outdoor as well as in indoor environments.

1.1 Goal

The goal of this diploma thesis is to implement a system which can localize a robot using no other sensors than a camera. This limitation was purposely chosen as the system will be used by future robotic students at the HTBLuVA (Technical Secondary College) and many robot systems used in the field of education are only poorly equipped with sensors that are able to detect its environment. One sensor used in the field of educational robotics is the either already equipped, or easily mountable camera.

As part of this thesis the authors not only want to implement an easy to use API for future robotic students, but to also show the possibilities and advantages of machine learning in localisation.

In order to accomplish precise localisation in various different surroundings, the authors plan on implementing a neural network. The neural network should take images, taken by the

camera, as an input, and outputs the relative distance to any object shown in the images. By using machine learning the system should be less dependent on a specific situation or setup in comparison to different camera based localisation methods. For example the localisation should work on objects varying in size and shape, as well as in different situations of lighting.

1.2 Motivation

In July 2019 the two authors of this work participated in the aerial tournament at the Global Conference on Educational Robotics held in Norman, Oklahoma. One of the two main challenges encountered at this tournament was landing a drone next to some randomly placed object, which colour, shape and size was known in advance.

The second challenge the participants at the tournament faced was flying from one side of randomly placed cardboard boxes to the other. The cardboard boxes, representing a mountain, are placed in one of various configurations, one of which can be seen in figure 1.1.



Figure 1.1: Seven cardboard boxes, representing a mountain, are placed in a random configuration. The team scores points if the drone passes the mountain while staying under the height limit indicated by the red dotted line.

The drones used at this aerial tournament are equipped with a camera, while lacking any other sensor that can be used to detect the obstacles and game items. Therefore the participants needed to be able to detect the distance to the object and the cardboard boxes using only the camera. At the Global Conference on Educational Robotics the authors of this work decided to detect the object based on its colour, but had to invest quite some time tweaking the values to get the localisation working correctly. Therefore the authors want to research and implement a method that is more robust than the colour based one.

1.3 Outlook and Perspective

The objective of this work is to create a system which uses machine learning methods in localising objects. After having trained the system, it should reliably return the x, y and z distances to an object, shown in two pictures taken from different angles. If this task turns out to be too complex the system should be simplified by only returning one output number corresponding to distance from the drone to the object.

It is planned that the distance will be measured from the second camera position to the centre of object, as seen in Figure 1.2.

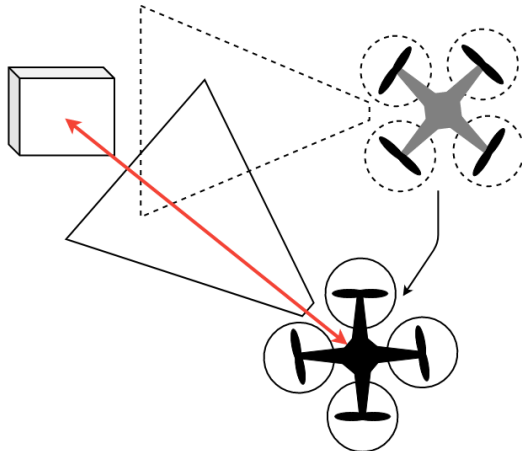


Figure 1.2: A drone tries to gather the data needed for the localisation of an object. After taking the first picture (grey drone with dotted lines) the drone flies to a second position (black drone with solid lines) to take another picture from a different point of view. The red line indicates the distance vector to be returned.

1.4 Equipment

Testing of the functionality of the localisation is to be performed on a Parrot Bebop 2. This drone was chosen as it is available to the authors during their time of research on this subject. This drone offers 1080p full HD video, which is believed to be more than sufficient for this project.

The Parrot Bebop 2 weighs 500g. The drone was not designed to carry any additional weight, therefore mounting a stereo camera, a LIDAR sensor or any other method of localisation using additional hardware is not recommended.

A wide-angle 14 megapixel fish-eye lens is mounted as a camera on the Parrot Bebop 2¹. It films 180 degrees vertically and horizontally and returns a 16:9 section which can be selected by specifying the vertical and horizontal angle of the virtual 16:9 camera. While the video resolution is limited to 1920 x 1080 pixels at 30 fps, the photo resolution is 4096 x 3072 pixels. A picture of the Parrot Bebop 2 can be seen in Figure 1.3.

¹Parrot Drones SAS. *Parrot Bebop 2 Specifications*. 2019. URL: <https://www.parrot.com/us/drones/parrot-bebop-2>.



Figure 1.3: The drone chosen for testing of the localisation system is a Parrot Bebop 2. It consists of four propellers each attached to a motor, a camera in the front, a battery located on the rear, some processors and a plastic frame to hold everything together.

It is assumed that the distance estimation using the system described in this thesis will work on various robotic systems. However, it will only be tested on this specific drone as other drones with a similar camera setup will behave similarly.

Chapter 2

Study of Literature

Author:

2.1 Different Approaches to the Problem

Localising a robot in an unknown surrounding can be achieved by a multitude of different sensors. To name a few stereo cameras, LIDAR systems, ultrasonic sensors and time-of-flight cameras all measure the distance to the objects located around the robot. This data can then be used to gather information about the current location of the robot or aid navigation.

2.2 Stereo Camera

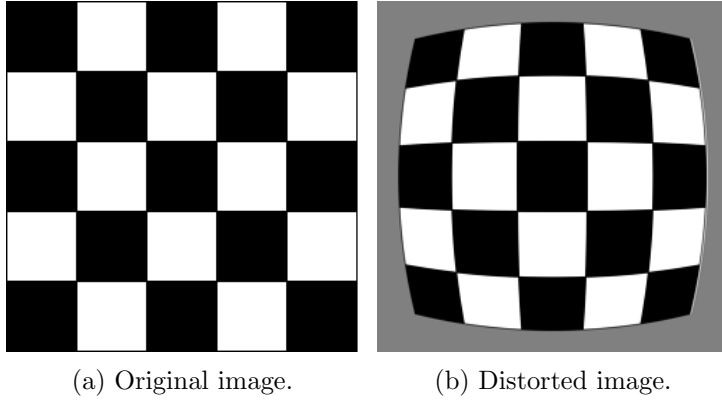
The challenge of sensing distances to various objects has been solved using stereo vision cameras. Computer stereo vision systems use two horizontally displaced cameras to take two images which are then processed together to gather the information on the depth of the images. This process can be rather complicated as the distortions of the images have to be undone, before the two images can be projected onto a common plane, a disparity map can be created by comparing the two images and a 3d point cloud can be generated from this comparison. In most robotics applications this point cloud is then filtered in search of some object, which distance was sought-after.

2.2.1 Distortion

One of the distortions that have to be undone before the images can be processed any further is called barrel distortion. It occurs when the lens used by the camera has a higher magnification at the centre of the image than at the sides. This distortion can be visualized as seen in Figure 2.1.

Gribbon et.al.¹ propose equations, which calculate the pixel values in the undistorted image based on the pixel values in the distorted image.

¹Donald G. Bailey K.T. Gribbon C.T. Johnston. “A real-time FPGA implementation of a barrel distortion correction algorithm with bilinear interpolation”. In: *Image and Vision Computing New Zealand*. 2003, pp. 408–413.



(a) Original image. (b) Distorted image.

Figure 2.1: The left shows the original image composed of straight horizontal and vertical lines. On the right image the effect of the barrel distortion can be seen. The distortion causes the lines to curve toward the outside of the image, causing the lines to appear in a barrel like shape.

In comparison to barrel distortion tangential distortion displaces points along the tangent of a circle placed at the centre of the image as seen in Figure 2.2.

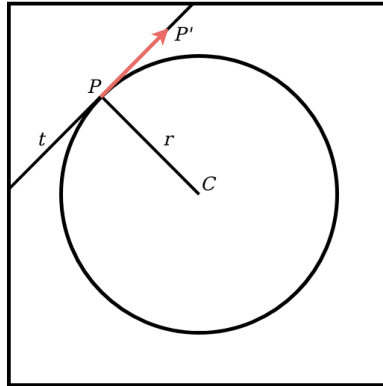


Figure 2.2: A point P is distorted along the tangent t of a circle placed at the middle of the image C with a radius r to a point P' . Distortions of this form are called tangential distortions.

The radius of the circle in Figure 2.2 is dependent on the point P . It can be calculated as the length between P and C . The length of the vector PP' is not uniform for all points and therefore depends on point P .

2.2.2 Image Rectification

Image Rectification projects multiple images taken from different points of view onto a common plane.

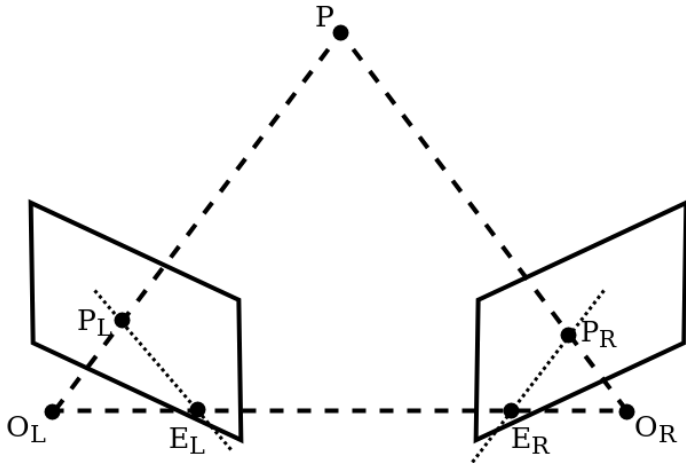


Figure 2.3: Two images containing some point P are taken from the two points O_L and O_R . Point P is projected in the image planes as points P_L and P_R . E_L and E_R depict the epipoles.

Chan et. al. propose an image rectification algorithm², which follows the following sequence of events:

1. At least seven matching points visible on both images are found.
2. The fundamental matrix (as well as the epipoles) are estimated.
3. The common region is identified (using epipolar geometry constraints).
4. The epipolar line is transferred and the Bresenham algorithm³ is used to extract pixel values.
5. The rectified image is resampled.

2.2.3 Disparity Map

A disparity map represents the depth of an image. It can be calculated by comparing the position of pixels in two images made for example by a stereo camera. Objects, that are closer, have a larger difference in their relative position on the two images, than objects that are farther away.

One approach, which focuses not only on the quality of the disparity, but also on the time needed to compute the result, is described in the work of Mühlmann et.al⁴.

²Hung Tat Tsui Zehzhi Chen Chengke Wu. “A new image rectification algorithm”. In: *Pattern Recognition Letters* 24.1-3 (2003), pp. 251–260.

³Jack Bresenham. “A linear algorithm for incremental digital display of circular arcs”. In: *Communications of the ACM* 20.2 (1977), pp. 100–106.

⁴Karsten Mühlmann et al. “Calculating Dense Disparity Maps from Color Stereo Images, an Efficient Implementation”. In: *International Journal of Computer Vision* 47.1 (Apr. 2002), pp. 79–88. ISSN: 1573-1405. DOI: 10.1023/A:1014581421794. URL: <https://doi.org/10.1023/A:1014581421794>.

2.2.4 3D Point Cloud

To generate a 3D point cloud out of the disparity map a two dimensional image has to be converted into a three dimensional space. This is done by extracting the information about the depth for each pixel from the disparity map. In our use case the resulting 3d point cloud then has to be filtered in search of the object, which distance to was sought after.

2.3 LIDAR

A lidar is a sensor that can be used to gather information about the environment. The sensor sends out light in a particular direction. Then the time needed for the light to return to the lidar is measured and the distance is calculated from that. By sending and receiving the light from multiple different directions data points from the entire two or three dimensional surrounding can be detected.

One example of a use case for a lidar sensor is demonstrated in the paper on Lidar-based teach-and-repeat of mobile robot trajectories of Spunk et al.⁵. The objective of their work is to teach a robot some trajectory by demonstration and then have the robot repeat the same trajectory as closely as possible. Their use of a lidar sensor enables them to follow the given trajectory with an accuracy of a few millimetres.

2.4 Structure from Motion

Similar to a stereo camera structure from motion estimates the three dimensional structure of the surrounding from the information of two dimensional images. The difference lies in the number of images typically used. While stereo cameras use two images, structure from motion commonly takes more images to reconstruct the three dimensional scene.

Structure from Motion can be used whenever it is necessary to take multiple images. This can be the case when one image can not include all of the relevant data that should be processed, for example when modelling terrain.

2.5 Depth Maps from Structured Light

By taking an image of an specially illuminated scene the structured light approach is able to calculate a depth map. Scharstein et al. present an approach that constructs high accuracy depth maps without the need to calibrate the light sources.⁶ So get information on specific distances to objects additional data, such as a different sensor measuring the distance to some (other) point in the image, is needed.

⁵Christoph Sprunk et al. “Lidar-based teach-and-repeat of mobile robot trajectories”. In: *2013 IEEE/RSJ International Conference on Intelligent Robots and Systems*. IEEE. 2013, pp. 3144–3149.

⁶Daniel Scharstein et al. “High-accuracy stereo depth maps using structured light”. In: *2003 IEEE Computer Society Conference on Computer Vision and Pattern Recognition, 2003. Proceedings*. Vol. 1. IEEE. 2003, pp. I–I.

2.6 Human Depth Perception

In medicine depth perception defined as the ability to see three dimensional space and judge distance accurately. Humans achieve depth perception by combining information from multiple depth cues. A depth cue is a feature of the environment or the person itself, that can be used to judge distance to objects. Depth cues can be classified in either of two categories: binocular and monocular, where binocular depth cues require two eyes and monocular only require one eye to work.

Which depth cue is used by humans in which situation was researched by Schrater et al.⁷.

binocular depth cues	
retinal disparity	Because the two eyes of a human person are separated by a few centimetres each eye perceives the environment from a slightly different point of view. These differences in the position of objects on the retina can be calculated as described by Cormack et al. ^a .
convergence	To focus on objects farther away the eyes have to be less crossed than when focusing on near objects. It is debatable whether the information on how crossed the eyes look is used by all humans to gather information on depth. Richards et al. designed a test and found that approximately two thirds of the population can use convergence as a depth cue. ^b

Table 2.1: A short overview of different binocular depth cues used by humans to see three dimensional space and judge distance.

^aRobert Cormack et al. “The computation of retinal disparity.” In: *Perception & Psychophysics* (1985).
^bWhitman Richards et al. “Convergence as a cue to depth”. In: *Perception & Psychophysics* 5.5 (1969), pp. 317–320.

monocular depth cues	
accommodation	As the eye focusses on an object the lens changes its thickness. The difference in thickness may be used to determine distance similar to convergence.
light and shadow	The position on which a shadow of an object falls can give information on its position in three dimensional space. This phenomenon can be observed in Fig. 2.4.

Table 2.2: A short overview of different monocular depth cues used by humans to see three dimensional space and judge distance.

⁷Paul R Schrater et al. “How optimal depth cue integration depends on the task”. In: *International Journal of Computer Vision* 40.1 (2000), pp. 71–89.

monocular depth cues	
linear perspective	Parallel lines in the environment, such as railroad tracks, appear to converge in one point. Therefore when shown an image containing converging lines, such as Fig. 2.4, the two dimensional picture conveys depth. Yonas et al. performed an experiment, showing at what point in their life infants develop the ability to use linear perspective. ^a
texture gradients	According to Ganong ^b the retina takes up two thirds of the inner side of the eyeball. It is covered with cone cells, which are able to detect light. Since the retina only contains a finite number of cone cells, which are placed some distance apart, the eye can only detect its surrounding at a limited resolution. Therefore objects farther away seem smoother as fine details can not be detected as easily.
overlap	Overlapping is a depth cue humans develop early in their life. It is described as getting information on the order of objects sorted by their distance by looking at the way objects hide parts of other objects. Hagen tested sensitivity of overlapping as a depth cue in three, five and seven year old children and found that all were able to perceive depth based on this information. ^c
aerial perspective	Very far distanced objects may appear hazy in certain weather conditions. The distance to these objects can be estimated by the haziness at which they appear.
relative motion	When the observer changes position the position at which objects are sensed change. The distance the objects change position in the eyes of the observer can be used to determine how far it is away. Closer objects move further while farther objects move less when the observer moves. This depth cue is called relative motion or motion parallax. According to Rogers et al. humans can reliably reconstruct distance from relative motion alone. ^d

Table 2.3: A short overview of different monocular depth cues used by humans to see three dimensional space and judge distance.

^aAlbert Yonas et al. "Infants' distance perception from linear perspective and texture gradients". In: *Infant Behavior and Development* 9.3 (1986), pp. 247–256.

^bMD William F. Ganong. *Review of Medical Physiology*. Appleton and Lange, 1997.

^cMargaret A Hagen. "Development of ability to perceive and produce pictorial depth cue of overlapping". In: *Perceptual and Motor Skills* 42.3 (1976), pp. 1007–1014.

^dBrian Rogers et al. "Motion parallax as an independent cue for depth perception". In: *Perception* 8.2 (1979), pp. 125–134.

2.6.1 Depth Sensation

Since it is not clear to what extent animals and infants can determine depth and sense their three dimensional environment the term depth perception is not used. It has been shown however that at least some animals can sense depth and therefore experience depth sensation.

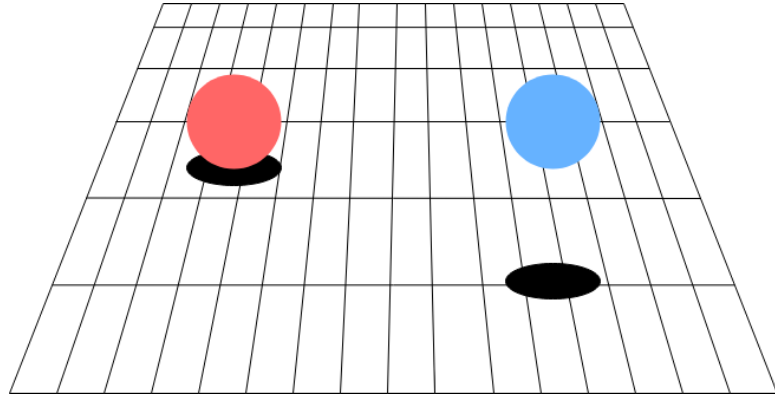


Figure 2.4: A two dimensional image conveying depth using linear perspective. The blue sphere seems closer than the red one, because of its shadow. Meanwhile the red sphere appears bigger as it is farther away and has the same relative size in the two dimensional image.

One experiment which tests depth sensation is called visual cliff.⁸ The task of the test subjects is to identify a sharp drop over which they must move to reach a desired destination. The setup of the experiment can be found in Fig. 2.5. It has been shown that infants along with all tested animals stop as soon as they have reached the cliff. Therefore they must experience some sort of depth sensation.

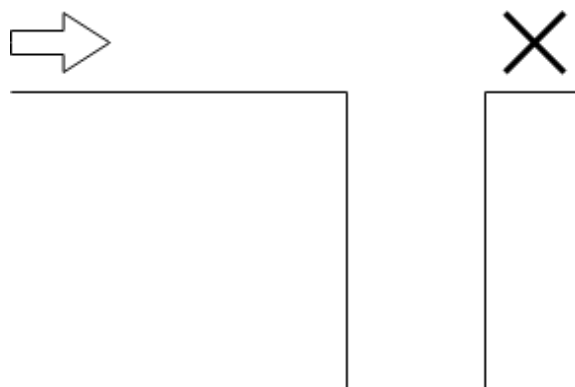


Figure 2.5: Setup of the visual cliff experiment. The arrow marks the starting point of the test subject. At the position of the X a desirable object is placed. Therefore the test subject starts moving toward the goal. If the subject has depth sensation it will stop before the cliff, while subjects without depth sensation won't be able to detect the cliff and therefore won't stop.

⁸Eleanor J Gibson et al. "The visual cliff". In: *Scientific American* 202.4 (1960), pp. 64–71.

Chapter 3

Methodology

Author:

3.1 Challenges in the Use of Stereo Cameras

Since many drones used in educational robotics can only carry a limited amount of weight it is not possible to attach a stereo camera to such a robot. Instead the functionality of a stereo camera on such a drone system can be mimicked by taking the first image, flying to a second position, located horizontally next to the first one and taking the second image. This process is not as precise as a stereo camera, where the two lenses are always positioned at an exact interval from one another. Therefore the output of this system might not work as reliable. Additionally other factors, such as differences in the two images due to some time passing between the taking of the images can have an effect on the accuracy.

Therefore the authors try to approach this challenge from the machine learning point of view. Neural networks can be taught to work with different changes in the environment and still return results with superior quality as opposed to a conventional implementation.

3.2 Generating Data

Neural Networks require huge amounts of data to work reliably. Because of the author's limited time frame this test data will be generated with the help of Blender 2.8. Blender is a free program for designing and animating 3D objects, which also supports scripting with Python to add or remove objects from a scene. The authors will use this capability to generate the huge amounts of test data needed from the perspectives of the two cameras, which point to a specific object in the scene. This enables the authors to create enough images to train a neural network, since shooting the amount of pictures needed by hand would take too long to consider.

3.2.1 Blender

Besides 3D-modelling Blender enables the user to perform various different actions, such as laying out scenes, UV-Editing, shading, animating and rendering. Additionally scenes can

be modified by executing Python scripts. Figure 3.1 shows the interface of Blender 2.8 with the default file loaded.

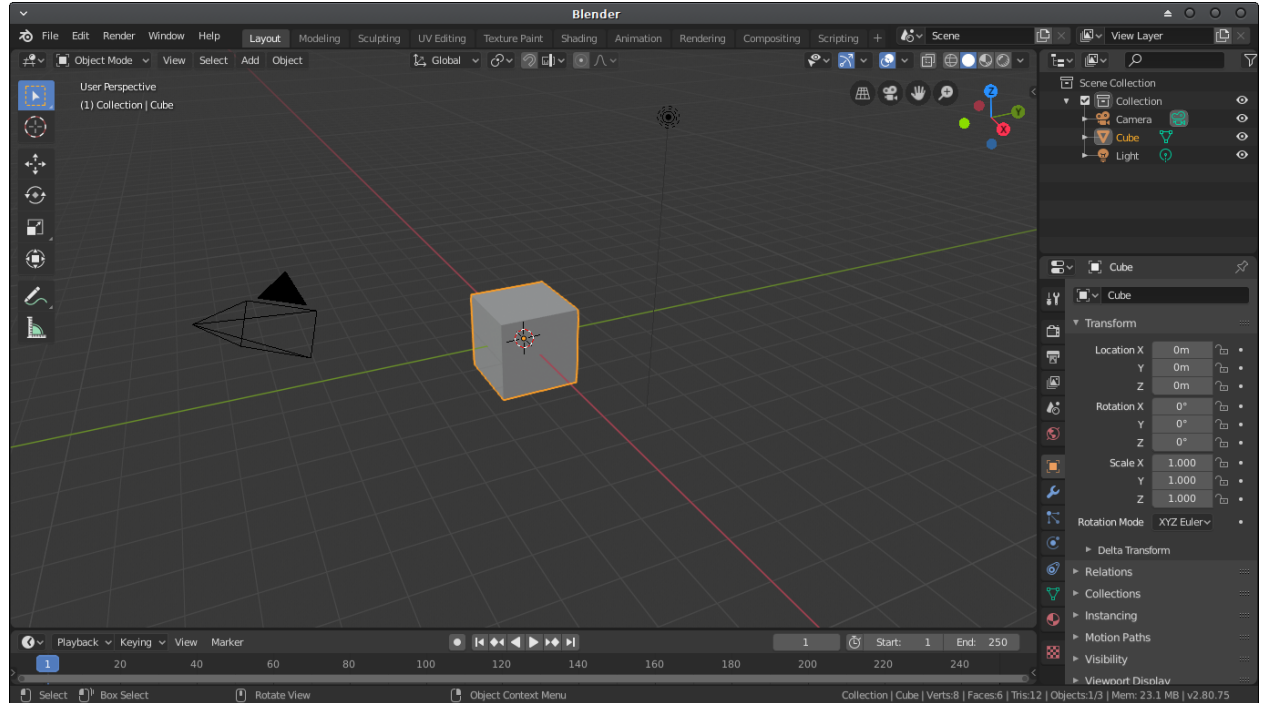


Figure 3.1: Blender interface after startup. The default scene features a grey cube, a camera (left of the cube) and a light source (black dot and circle positioned on the top right of the cube).

The authors decided to extensively use the scripting function in their work. One example of a Python script, that can be executed in Blender is the following code:

```

1 import bpy
2
3 # Selects all cubes and deletes them
4 bpy.ops.object.select_all(action='DESELECT')
5 bpy.ops.object.select_by_type(type='MESH')
6 bpy.ops.object.delete()
7
8 # Adds a new cube
9 bpy.ops.mesh.primitive_cube_add(size=3, enter_editmode=False, location=(4, 2, 0))
10
11 # Adds a new material representing the colour red
12 bpy.ops.material.new()
13 material = bpy.data.materials[-1]
14 material.name = 'Red'
15 material.diffuse_color = (0.8, 0.1, 0.1, 1)
16

```

```
17 # Apply material onto the newly created cube object  
18 bpy.context.active_object.data.materials.append(material)
```

This code first clears the scene from other meshes (running the script twice would otherwise place the new cube inside the old cube). Then a new mesh in form of a cube is added at the given location. Next colour is added to the new cube by applying a material. A material is a specification of how the surface of the object should look. Advanced materials can represent raw or reflective surfaces, however the authors decided to keep it simple. The chosen material represents a red surface (the red/green/blue/alpha channels ranging from 0.0 (for 0) to 1.0 (for 255) are specified). Lastly the created material is applied to the object. The final result can be seen below:

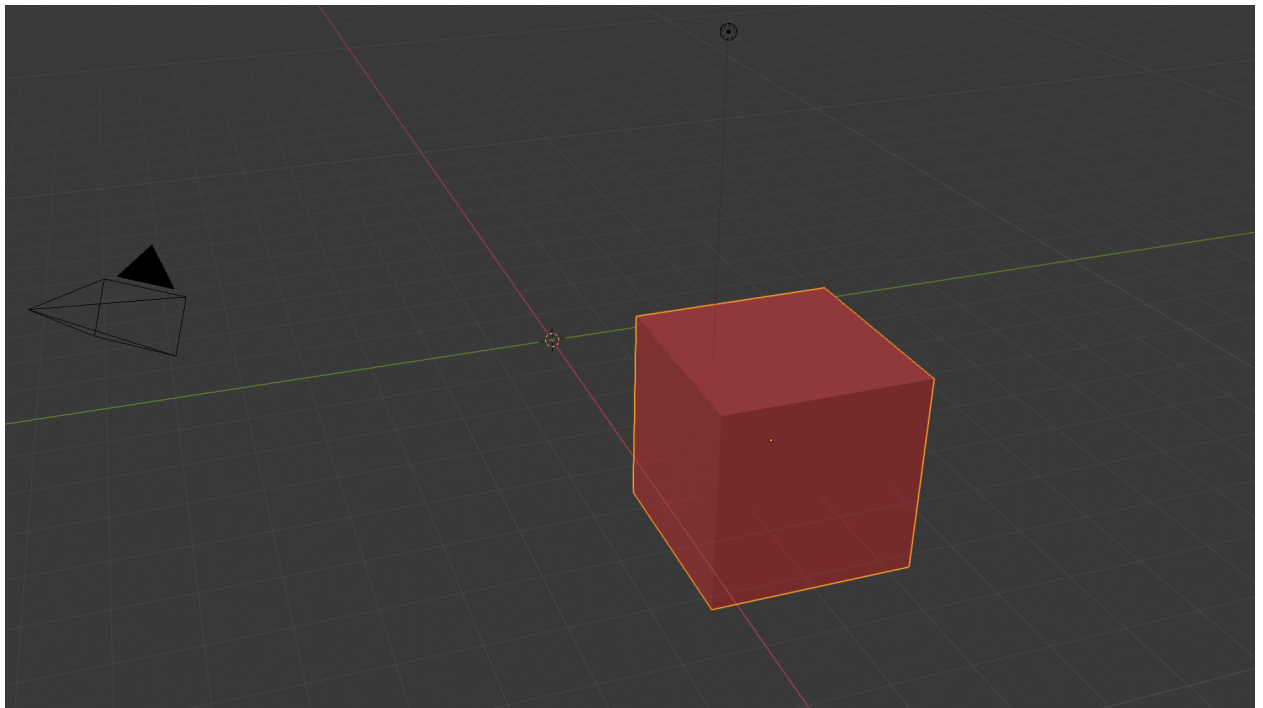


Figure 3.2: The result of the above code. After the default cube is deleted, a new one is added with a red material and translated via the 'location' argument.

Using similar Python scripts the authors will generate the image data necessary as well as perform the calculation of the distance which will be specified as the correct values to train the neural network on.

3.3 Image Preprocessing

After the test images have been rendered with the help of Blender some image preprocessing is required. For example the machine learning component of this project should take two images as an input. To simplify the input the two images will be placed next to each other

to form a new image twice as wide as the original images. This process is visualized in Figure 3.3. Other preprocessing measures that have to be taken are downscaling the image, as to not have too many weights in the first layer of the neural network.

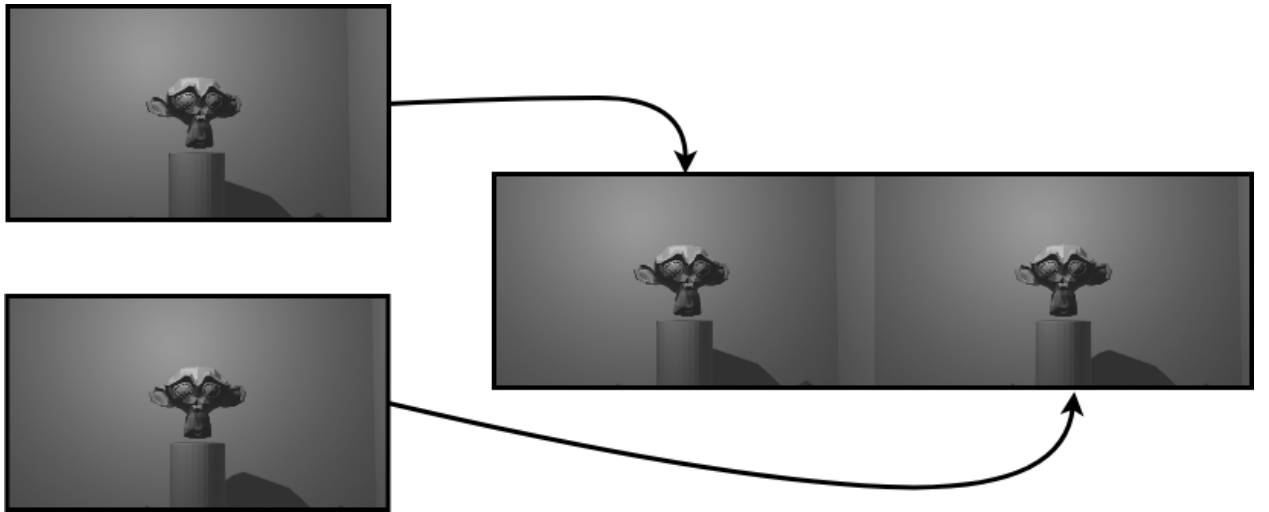


Figure 3.3: Two greyscale renders showing the same object from two different camera positions in Blender are merged into one picture which can be feed into the neural network component.

Additionally, the authors decided to experiment if manipulating these test images further would result in differences of distance perception by the neural network or if they would speed up or slow down the learning phase. These manipulations are done using OpenCV and Python3. OpenCV provides many image manipulation tools. For this project the authors chose the following methods of image manipulation:

Name	Description
Greyscale	A greyscale image is an image with only one value for the red, green and blue colour channels, resulting in different shades of grey instead of usual colours.
Resolution	Resolution refers to the number of pixels placed in each dimension (width and height).
Cropping	When cropping an image an unwanted part located at the peripheral areas of the image is removed.
Saturated	Saturated images feature stronger colours, which makes them easier to distinguish from another.
Brightness	Brightening images can make colours harder to distinguish from another. Additionally it can lead to the same problems encountered in overexposed images, such as part of the image being completely white and therefore not providing any information.

3.4 Neural Network

A neural network is a tool used in machine learning. It consists of nodes, each receiving some input values as well as some weights associated to each input value and outputs some output value. The calculation returning the output value is relatively simple. Many of these nodes form what is called a layer. By forming multiple connections between the nodes the neural network can perform more complex tasks. A vanilla neural network consists of multiple layers, where each node receives all output values of all nodes in the previous layer as an input. A visualization of a vanilla neural network can be seen in Figure 3.4. By manipulating the weights associated to each input value the network can learn to solve a given task.

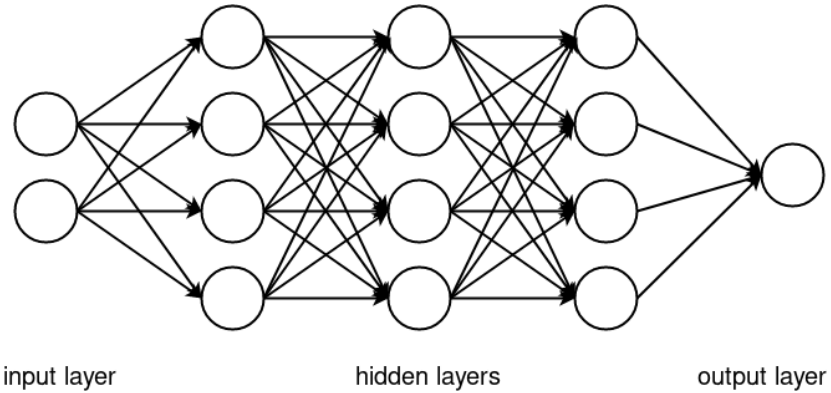


Figure 3.4: Depiction of a vanilla neural network. Each circle represents a node and the arrows show the flow of information. All nodes on the same level are collectively called a layer.

3.4.1 Convolutional Neural Network

One of the disadvantages of neural networks is that they need huge amounts of data in order to optimize the values of all weights. Therefore a modified version of neural networks was invented. Convolutional neural networks simplify the optimization of the weights by stating that some weights are shared between multiple connections of nodes. This results in fewer weights having to be optimized. Additionally convolutional neural networks perform similar actions in multiple parts of the input data which especially makes sense when working with images, e.g. search for edges in all sections of an image.

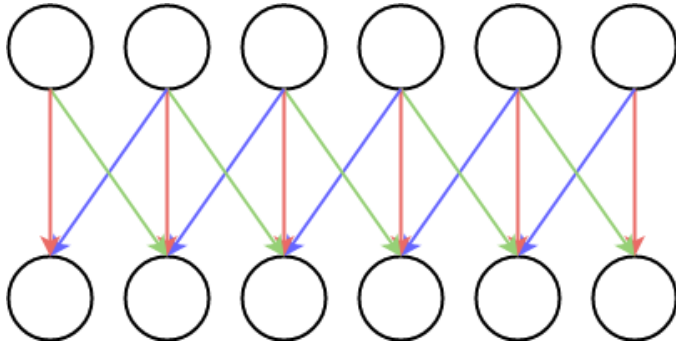


Figure 3.5: Segment of a convolutional neural network. In comparison to a vanilla neural network each node is only connected to its closest neighbours. Additionally all arrows connected to another node in the same relative position (same colour) have the same weight attached.

3.4.2 Loss Function

A loss function is used in optimization problems to determine the loss or cost of some operation. Therefore a low loss is desired. Some loss functions commonly used in machine learning are:

Mean Squared Error

$$mse = \frac{1}{n} \sum_{i=1}^n (x_i - \hat{x}_i)^2$$

where n is the number of elements, x is the correct value and \hat{x} is the estimated value. Squaring the difference of the correct and estimated value is necessary, as negative and positive differences could otherwise annul each other.

Mean Absolute Error

$$mae = \frac{1}{n} \sum_{i=1}^n |\hat{x}_i - x_i|$$

where n is the number of elements, x is the correct value and \hat{x} is the estimated value. In comparison to the mean squared error, this method uses the absolute value of the difference.

Mean Absolute Percentage Error

$$mape = \frac{100\%}{n} \sum_{i=1}^n \left| \frac{x_i - \hat{x}_i}{x_i} \right|$$

where n is the number of elements, x is the correct value and \hat{x} is the estimated value. The mean absolute percentage error returns the average percentage by which the estimated value differs from the actual one.

Mean Squared Logarithmic Error

$$msle = \frac{1}{n} \sum_{i=1}^n \log(\hat{x}_i + 1) - \log(x_i + 1)$$

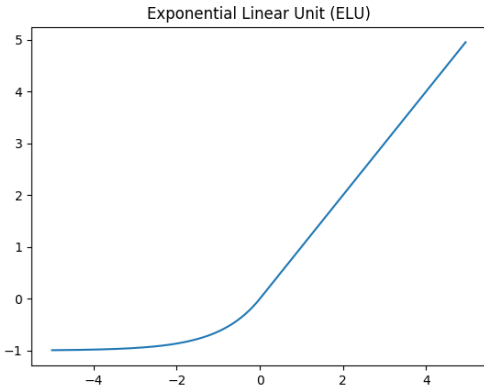
where n is the number of elements, x is the correct value and \hat{x} is the estimated value.

Logcosh

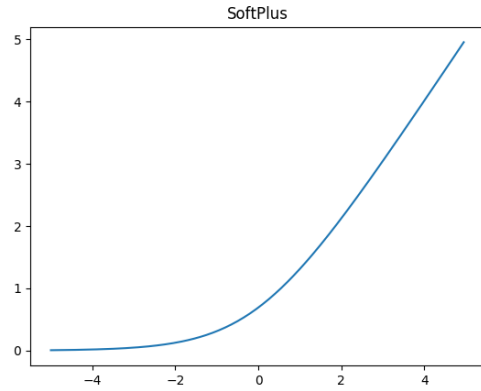
Kullback Leibler Divergence

3.4.3 Activation Function

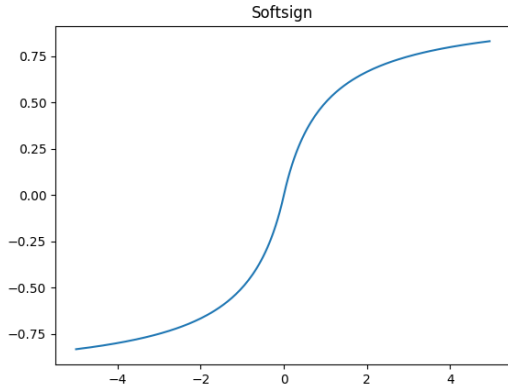
The activation function defines the output of a node based on the input values it receives. Some of the most widely used activation functions are displayed in Fig. 3.6 and Fig. 3.7.



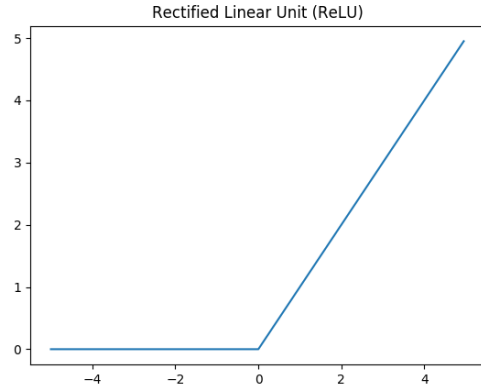
(a) The Exponential Linear Unit function is defined as $f(\alpha, x) = \begin{cases} x & x \geq 0 \\ \alpha(e^x - 1) & x < 0 \end{cases}$.



(b) The SoftPlus function is defined as $f(x) = \ln(1 + e^x)$.



(c) Softsign is defined as $f(x) = \frac{x}{1+|x|}$.

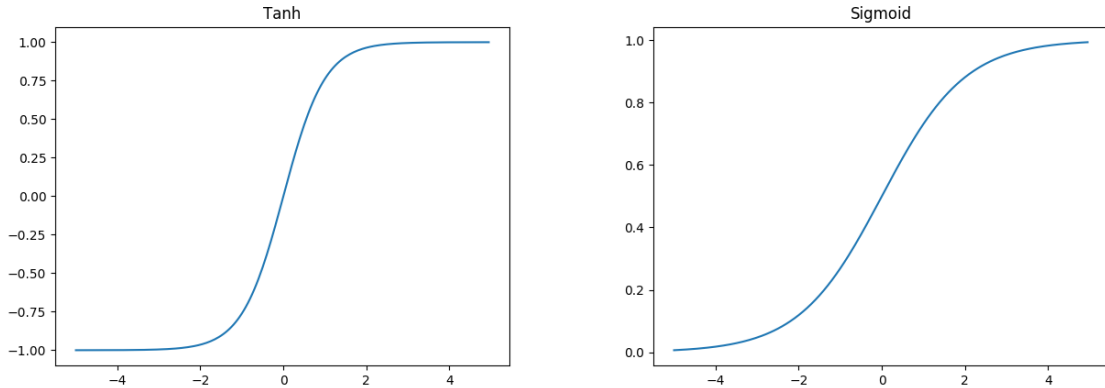


(d) Rectified Linear Unit can be described as $f(x) = \begin{cases} x & x \geq 0 \\ 0 & x < 0 \end{cases}$

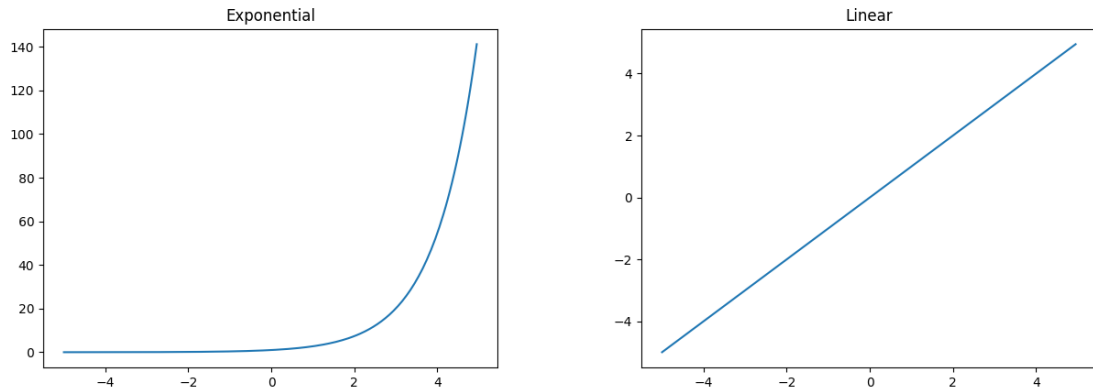
Figure 3.6: An excerpt of the most common activation functions used in machine learning. The rest can be found in Fig. 3.7. Non-linear functions allow the neural network to solve more complex tasks. All activation functions are plotted from -4 to 4 as the most interesting features of these functions often occur around 0.

3.4.4 Initializer

In neural networks the initial weights of all layers have to be set before training can begin. These weights can either be set to some constant value or initialized by random values from some distribution. Some basic initializer distributions are plotted in Fig 3.8 and Fig 3.9.



(a) The Tanh activation function is defined as $f(x) = \tanh(x)$. (b) The Sigmoid function is defined as $f(x) = \frac{1}{1+e^{-x}}$.



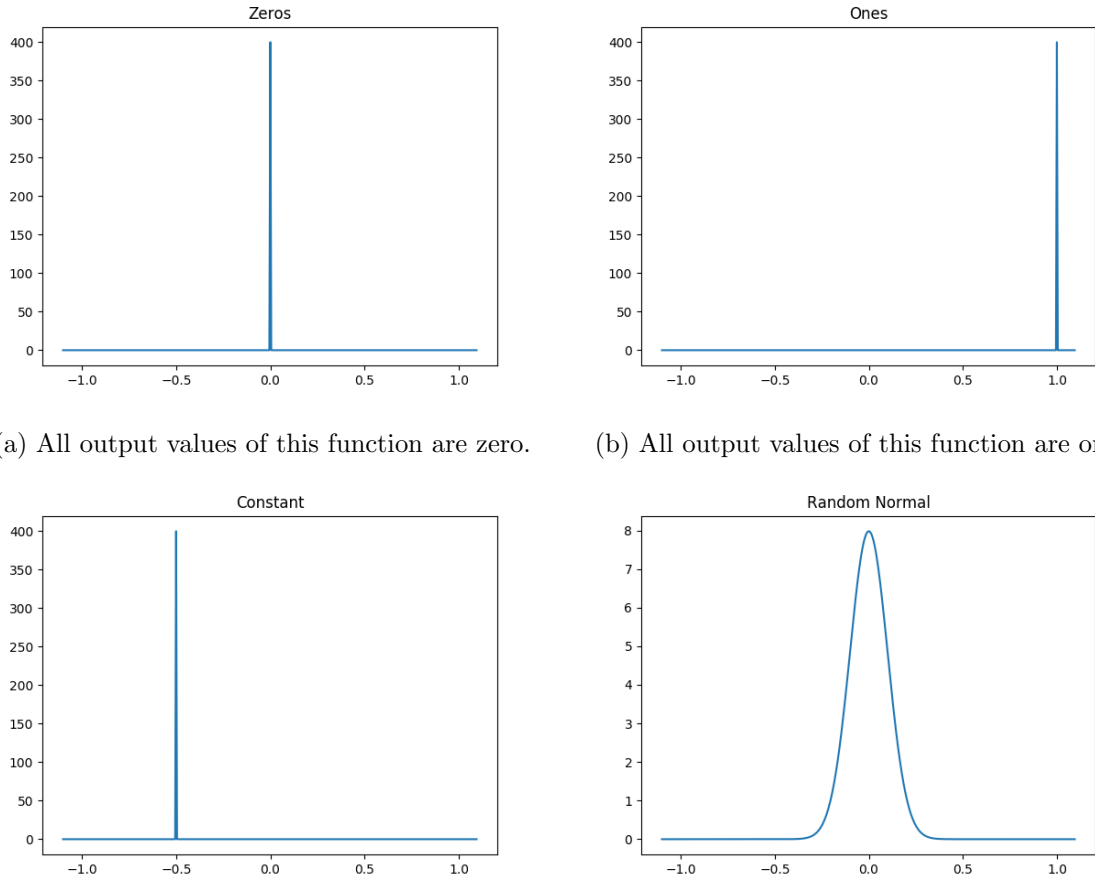
(c) The Exponential activation function is defined as $f(x) = e^x$. (d) The Linear activation function, also called identity function, is defined as $f(x) = x$.

Figure 3.7: Other common activation functions used in machine learning. Once again all activation functions are plotted from -4 to 4 for the same reason.

3.4.5 Optimizer

The objective of an optimizer is to optimize (find a local minimum of) the loss function. Some of the most widely used optimizers are:

- Stochastic gradient descent (SGD)
- Root Mean Square Propagation (RMSProp)
- Adaptive Gradient Algorithm (Adagrad)
- Adadelta
- Adaptive Moment Estimation (Adam)



(a) All output values of this function are zero.

(b) All output values of this function are one.

(c) All output values of this function are one constant value. In this example 0.5 was chosen as the output value.

(d) A random normal distribution where the mean is set to 0 and the standard deviation is set to 0.05. Values closer to the mean value are more likely.

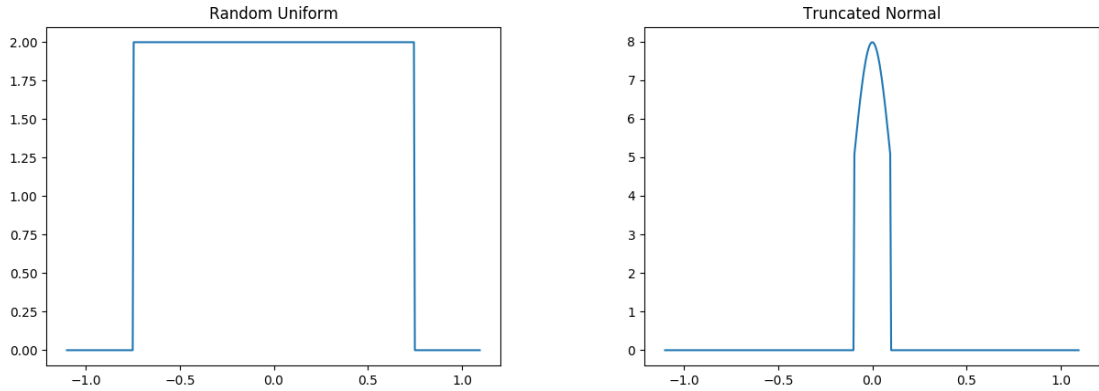
Figure 3.8: These are some of the most basic distribution most initializer functions are based on.

- Adamax
- Nesterov Adam (Nadam)

3.4.6 Overfitting and Underfitting

Overfitting occurs if the data sample is replicated too closely. One example of overfitting can be seen in Figure 3.10. The function used is a high degree polynomial function, which has a very good fit on the noisy data originating from a linear correlation, but when testing this model on other data points, especially far from zero on the x-axis it fails to represent the original relation.

The goal is to find a function, that has just enough complexity to fit the data points. The



- (a) In a random uniform function all values between the set minimum and maximum value are equally likely.
- (b) A distribution based on the normal distribution, where all values outside of two standard deviations away from the mean are redrawn.

Figure 3.9: More basic distribution initializer functions of weights and biases are often based on.

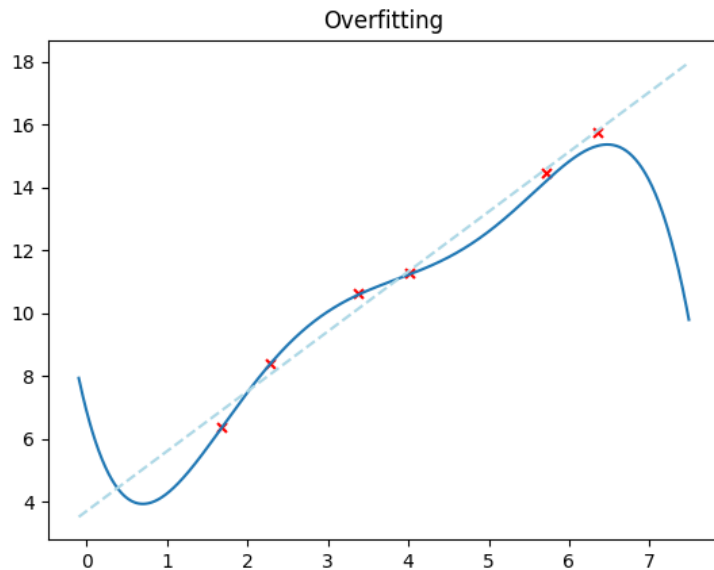


Figure 3.10: Noisy data points originating in a linear correlation (red crosses) are fitted using a high degree polynomial function (blue line), resulting in overfitting. A linear fit (light blue dashed line) has a worse fit on the given data sample, but gives better results when extrapolating.

opposite of overfitting is called underfitting. When underfitting a more complex problem is approximated using too simple methods, again resulting in poor results.

3.5 Neural Network Implementations

The authors decided to use a software framework called TensorFlow for the first implementation of the neural network. This has the following two advantages: using Tensorflow allows for a low effort proof of concept and it makes testing out different configurations (e.g. number of hidden layers or filters in image preprocessing) of the neural network easier.

After it has been shown that the challenge of detecting the distance to an object can be solved using machine learning, the authors plan on implementing a neural network in C++ on their own. The knowledge gained in the TensorFlow implementation will be used in the C++ implementation, which hopefully will make the work less time consuming.

3.6 TensorFlow

As machine learning has gained popularity in recent years the demand for applicable frameworks grew. One of the most popular is called TensorFlow. It was developed by Google for internal use and was published under the Apache License 2.0 on the 9th of November 2015. TensorFlow supports APIs for Python, C, C++, Go, Java, JavaScript and Swift. Due to its popularity third party APIs for C#, R, Scala, Rust and many more were developed.

Its use cases reach from categorizing handwritten digits to YouTube video recommendations, one of the many applications Google use it for.

Tom Hope et al. describe TensorFlow as a software framework for numerical computations based on dataflow graphs¹.

3.6.1 Computation graph

To compute a value using TensorFlow a computation graph has to be constructed. In this graph each node corresponds to an operation, such as subtraction or division. By connecting these nodes via edges the output of one node can be fed as input into another node. One example of such a computation graph can be seen in Figure 3.11.

The implementation of the computation graph, shown in Figure 3.11, in Python could look as follows:

```
1 import tensorflow as tf
2
3 a = tf.constant(28)
4 b = tf.constant(2)
5
6 c = tf.multiply(a, b)
7 d = tf.add(a, c)
8 e = tf.divide(d, b)
```

¹Itay Lieder Tom Hope Yehezkel S. Resheff. *Learning TensorFlow*. O'Reilly, 2017, page 6.

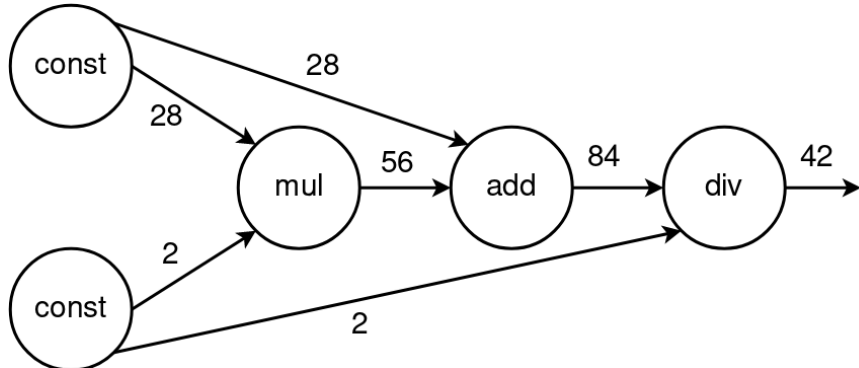


Figure 3.11: Each node represents an operation, where *const* stands for a constant value, *add* for addition, *mul* for multiplication and *div* for division. Edges, represented by arrows, connect nodes. The information shared between the nodes is described by the numbers written next to the edges. This computational graph calculates the result of the arithmetic expression $(28 * 2) + 28/2$.

```

9
10 with tf.Session() as sess:
11     out = sess.run(e)
12
13 print(out)

```

The first line specifies that the TensorFlow functionality should be imported. Line 3 and 4 define the two constant values and assigns them the values 28 and 2 respectively. In line 6 to 8 the other nodes of the graph are specified. E.g. in line 6 a new node, named *c*, is created and the output of node *a* and node *b* are connected as its input. To perform the calculation described by the graph a new session is created in line 10. Finally the output of the graph (node *e*) is specified in line 11, the result is calculated and printed in line 13.

TensorFlow allows for another way of specifying a graph with these arithmetic operations:

```

1 import tensorflow as tf
2
3 a = tf.constant(28)
4 b = tf.constant(2)
5
6 e = (a * b + a) / b
7
8 with tf.Session() as sess:
9     out = sess.run(e)
10
11 print(out)

```

This code is equivalent to the first one, but uses syntactic sugar to shorten line 6 to 8 in the first code block into line 6. At this point it should be noted that while it might look like it

line 6 does not calculate anything. It simply describes how the computational graph should look. The answer (42) is calculated in the session in line 9.

Using the same principle, but different functions TensorFlow allows the creation of complex neural networks in a simple fashion.

3.6.2 Alternatives to Tensorflow

TensorFlow offers some abstraction libraries, such as Keras. As some code snippets are used very frequently and with only slight variation when implementing a Neural Network, Keras offers these code blocks as predefined functions, making development easier for “standard” use cases.

For example Keras provides several different layers, that can be used to put together a neural network. Table 3.1 describes just some of the available layers.

Name	Description
Dense	regular densely connected layer
Activation	Applies an activation function to an output
Dropout	Applies Dropout to the input
Flatten	Flattens the input down to shape
Conv1D	1D convolution layer (e.g. temporal convolution)
MaxPooling1D	Max pooling operation for temporal data
LocallyConnected1D	Locally-connected layer for 1D inputs
SimpleRNN	Fully-connected RNN where the output is to be fed back to input

Table 3.1: Short description of layers available in Keras, that can be used to assemble a neural network, with little effort.

Another feature Keras offers is image preprocessing. In comparison to the authors use of this phrase, Keras offers transformations of the image that alter the image only slightly, which prevents overfitting, when using only a small input data set of images. Examples of the transformations offered are: rotating the image, shifting the image along the vertical or horizontal axis, changing the brightness of the image, zooming, flipping the image vertically or horizontally and rescaling the image.

Other machine learning frameworks are:

- PyTorch
- Caffe
- Microsoft Cognitive toolkit (CNTK)
- Caffe2
- MXNet
- Torch
- Theano
- DeepLearning4j

Chapter 4

ROS2

Author:

4.1 What is ROS?

[Ubuntu?]

[INFO: ROS (Robot Operating System) provides libraries and tools to help software developers create robot applications.¹]

[TEST: asdf²] [Core Concepts]

4.1.1 Nodes

[Wie verwenden wir das? / Wie macht es unsere Arbeit leicher?]

4.1.2 ...

4.2 Why use ROS?

4.3 Comparing ROS and ROS2

[python2 < python3]

¹Inc. Open Source Robotics Foundation. *Documentation - ros wiki*. 2019. URL: <https://wiki.ros.org>.

²Open Source Robotics Foundation, *Documentation - ros wiki*.

Chapter 5

Implementation

Author:

5.1 Generating test data

Good test data is of utmost importance in machine learning. The system can only know information that is depicted in the training data, which is why it is important to include as many aspects of the problem as possible in this data.

Since machine learning needs a lot of data in order to solve the given task it can be tiresome to generate and label all this data by hand. Therefore the authors decided to simulate the objects and the camera using a computer graphics modelling software called Blender.

Blender allows for relatively easy generation of training data by providing a Python API. With this API almost anything that can be done using the blender user interface can also be done using Python.

For generating data the first step for the authors was to model a scene, as seen in Figure 5.1. This scene would contain a building split into multiple rooms. Each of the rooms is home to one object, which was rendered using two cameras, representing two points of view. The first camera is positioned relative to the object, whereas the second camera is positioned relative to the first camera, guaranteeing a different view on the object. Lastly, the two renders formed one input for the neural network.

For the test objects the authors used two objects: a monkey head, which already exists in Blender and a self-modelled object, representing a vase with some decorating sticks in it. Both objects can be seen in Figure 5.2.

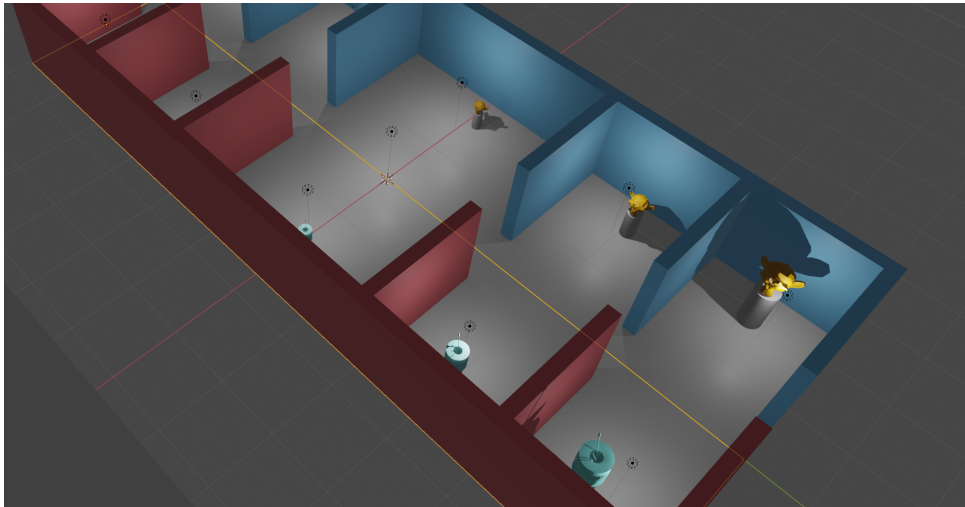
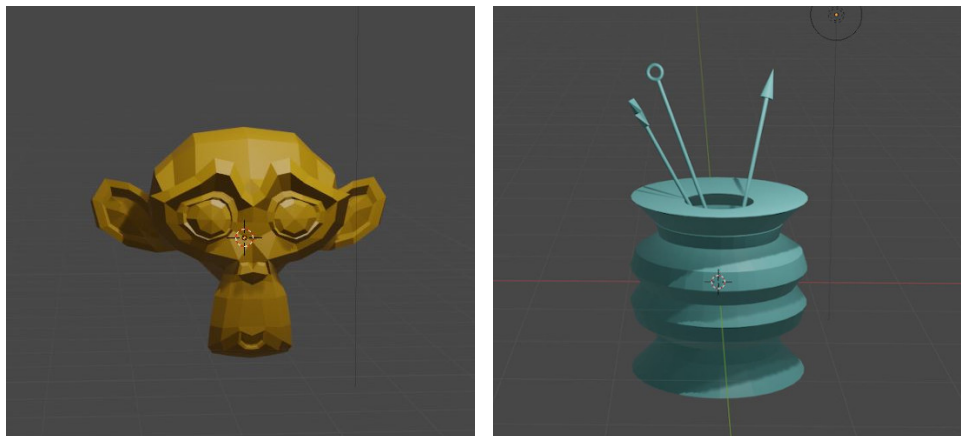


Figure 5.1: The test scene for generating data. Each object is placed in a room and is separated by walls.



(a) One of the test objects - a monkey head.
(b) One of the test objects - a decorative vase.

Figure 5.2: The two test objects as displayed in the Blender interface.

5.1.1 Generating the Render-Pairs

The following code generates the two needed renders for one of the test objects:

```

1 # Generate for 1 object
2 def generate_1(renderpath, infopath, target_name, iterations):
3     target_loc = bpy.data.objects[target_name].location
4
5     XMIN = target_loc.x - 0.6 if target_loc.x > 0 else target_loc.x + 0.6
6     XMAX = target_loc.x - 8.6 if target_loc.x > 0 else target_loc.x + 8.6

```

```

7 YMIN = target_loc.y - 1.85
8 YMAX = target_loc.y + 1.85
9 ZMIN = 0.75
10 ZMAX = 2
11
12 RENDERPATH = renderpath + target_name
13 INFOPATH = infopath + target_name
14
15 RENDERFILEPATH = RENDERPATH + "/{}-{}.jpg"
16 INFOFILEPATH = INFOPATH + "/{}-{}.txt"
17
18 make_dirs(RENDERPATH, INFOPATH)
19
20 for i in range(0, iterations):
21     # Calculate values
22     X = random.uniform(XMIN, XMAX)
23     Y1 = random.uniform(YMIN, YMAX)
24     Y2 = Y1 + 1 if (Y1 - target_loc.y) < 0 else Y1 - 1
25     Z = random.uniform(ZMIN, ZMAX)
26
27     # Add first camera
28     add_camera(X, Y1, Z, target_name)
29     write_dist_info(INFOFILEPATH, target_name, i, 1)
30     render(RENDERFILEPATH, i, 1)
31     del_cameras()
32
33     # Add second camera
34     add_camera(X, Y2, Z, target_name)
35     write_dist_info(INFOFILEPATH, target_name, i, 2)
36     render(RENDERFILEPATH, i, 2)
37     del_cameras()

```

This code can seem overwhelming at first, so the authors decided to explain each part of it. The first code block

```

1 target_loc = bpy.data.objects[target_name].location
2
3 XMIN = target_loc.x - 0.6 if target_loc.x > 0 else target_loc.x + 0.6
4 XMAX = target_loc.x - 8.6 if target_loc.x > 0 else target_loc.x + 8.6
5 YMIN = target_loc.y - 1.85
6 YMAX = target_loc.y + 1.85
7 ZMIN = 0.75
8 ZMAX = 2

```

stores the location of the given target, or object, in the variable 'target_loc'. Relative to this location the min/max values for the X/Y/Z coordinates are being calculated. These coordinates are used for the camera placement, so the camera is placed relatively to the object. 'YMIN', for example means, that the camera's Y value can be no further than 1.85m

to the left of the object. 'YMAX' clamps this value so there is a border on the right side as well.

```
1 # Calculate values
2 X = random.uniform(XMIN, XMAX)
3 Y1 = random.uniform(YMIN, YMAX)
4 Y2 = Y1 + 1 if (Y1 - target_loc.y) < 0 else Y1 - 1
5 Z = random.uniform(ZMIN, ZMAX)
```

This code block does exactly what was described before. A random value for X/Y/Z is chosen. Notice that the Y value is split in two, where 'Y1' uses 'YMIN' and 'YMAX' and 'Y2' uses 'Y1' for calculation. This is to guarantee a different angle to the object, because camera one will use 'Y1' and the second camera will use 'Y2'.

[TODO: Maybe add image illustrating above text]

```
1 # Add first camera
2 add_camera(X, Y1, Z, target_name)
3 write_dist_info(INFOFILEPATH, target_name, i, 1)
4 render(RENDERFILEPATH, i, 1)
5 del_cameras()

6
7 # Add second camera
8 add_camera(X, Y2, Z, target_name)
9 write_dist_info(INFOFILEPATH, target_name, i, 2)
10 render(RENDERFILEPATH, i, 2)
11 del_cameras()
```

This last code block is mostly the same for each camera. The first camera uses 'Y1' for its placement, centered on 'target_name' (the object). Then, from the location of the first camera, the distance to the object is calculated and written to a file. After the calculation of the actual distance blender renders an image from the first camera's point of view, after which the first camera is being deleted. This is the same for the second camera, except 'Y2' is used for its placement.

5.2 OpenCV

OpenCV is a framework for image manipulation. Some of its use cases are changing the colour spectrum, filtering the image by colour and cropping images. The authors use OpenCV to test whether there are differences between filters for the images in the training data, for example greyscale images compared to coloured images. An example render, which OpenCV gets as an input can be seen in Figure 5.3.

5.2.1 Greyscale

Converting an image into greyscale can easily be achieved by the following OpenCV code:



Figure 5.3: One of two original renders produced by Blender, both depicting the same object from different points of view.

```
1 import cv2
2
3 image = cv2.imread('path/to/image')
4 image_greyscale = cv2.cvtColor(image, cv2.COLOR_BGR2GRAY)
5 cv2.imwrite('path/for/saving/greyscale/image', image_greyscale)
```

This code first reads the image into 'image'. Then it converts the color of 'image' into a greyscale format and stores the result into 'image_greyscale', which is then written to the specified path. The output generated by this code is depicted in Figure 5.4.

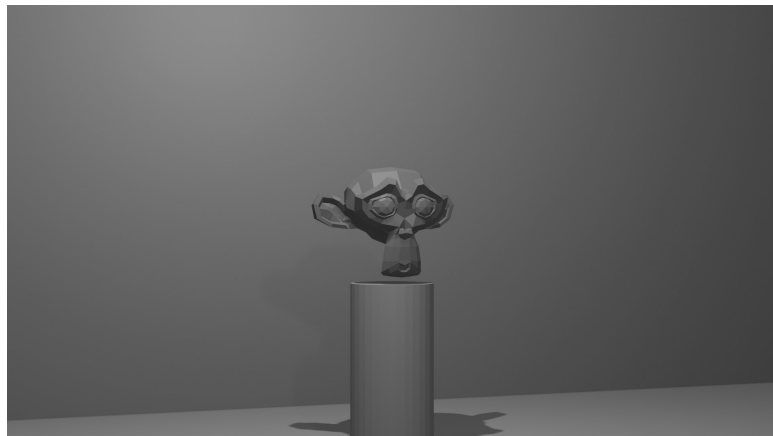


Figure 5.4: The greyscale image produced by OpenCV.

The advantage of using greyscale images in neural networks is the simplification of the input layer. In greyscale images each pixel can be represented by a single decimal value between 0 and 1. This enables the first layer of the neural network to be two dimensional instead of the

three dimensional counterpart, where each pixel is represented by the three decimal values for the red, green and blue colour channels.

5.2.2 Resolution

By reducing the resolution of an image the density of pixels is lessened. In this process information, that can not be regained, is lost. The OpenCV code for downscaling the images used by the authors is the following:

```
1 import cv2
2
3 image = cv2.imread('path/to/image')
4
5 scale_percent = 10 # percent of original size
6 width = int(image.shape[1] * scale_percent / 100)
7 height = int(image.shape[0] * scale_percent / 100)
8 dim = (width, height)
9
10 downscaled = cv2.resize(image, dim)
11 cv2.imwrite('{}{}'.format(newdir_path, filename), downscaled)
```

OpenCV provides a `resize` function, which takes an image and the new dimensions of the image as an argument and outputs the resized image. To make sure the aspect ratio stays the same new image dimensions are calculated as a percentage of the original ones.

The output image of this code can be found in Figure 5.5.



Figure 5.5: Image with lower resolution than the original one. Due to the fact that the image is displayed in the same size as Figure 5.3, the pixel size in this image appears larger.

Downscaling the images before they are passed into the neural network can be profitable, because the number of weights in the first layer of the network is reduced. This can advance the learning speed.

5.2.3 Cropping

Cropping an image can remove unnecessary or unwanted parts of an image by simply cutting off areas. This is often wanted in photography to only keep what is interesting in a photo and to shift the view of the viewer to specific areas. However, the authors guess that cropping an image will worsen performance of the neural network, because information of the relative sizes is partly lost. It compares to zooming into the image.

Such a cropped image produced by the following code can be found in Figure 5.6.

```
1 import cv2
2
3 image = cv2.imread('path/to/image')
4
5 crop_margin_percent = 5
6 crop_margin_width = int(image.shape[1] * crop_margin_percent / 100)
7 crop_margin_height = int(image.shape[0] * crop_margin_percent / 100)
8
9 crop_img = image[crop_margin_width:-crop_margin_width, crop_margin_height:-
    crop_margin_height]
10 cv2.imwrite('{}/{}'.format(newdir_path, filename), crop_img)
```



Figure 5.6: In this image five percent of each side was removed, therefore the object appears closer if the image is displayed in the same size. Some information positioned in the outer areas of the image are lost during the cropping process.

5.2.4 Saturated

A saturated image means stronger colours, making them more distinguishable from each other. If an image is not saturated enough, colours appear as "washed out" and differences in colour are difficult to determine. Therefore, in order to help the neural network, the authors decided to also test with saturated versions of these images.

```
1 import cv2
```

```

2
3 image = cv2.imread('path/to/image')
4
5 hsv = cv2.cvtColor(image, cv2.COLOR_BGR2HSV).astype('float32')
6 (h, s, v) = cv2.split(hsv)
7 s *= 1.5
8 s = np.clip(s, 0, 255)
9 hsv = cv2.merge([h, s, v])
10 saturated = cv2.cvtColor(hsv.astype('uint8'), cv2.COLOR_HSV2BGR)
11 cv2.imwrite('{}{}'.format(newdir_path, filename), saturated)

```

To saturate an image using OpenCV it has to be converted into the HSV colour representation. The HSV representation specifies each colour as a hue, a saturation and a value. Therefore changing the saturation in this model is relatively easy, as the saturation value of each pixel can simply be multiplied by a constant. Before the image can be converted back into the bgr colour representation the saturation values are restricted between 0 and 255, the lowest and highest saturation possible. The result achieved by this code can be seen in Figure 5.7.



Figure 5.7: A saturated version of Fig. 5.3.

5.2.5 Brightness

Because the neural network should also work in different environment, where other methods could have problems, the authors also tested with overly bright images. This makes it very hard to notice dark areas, such as shadows, to help with distances between objects and scaling of objects.

```

1 import cv2
2
3 image = cv2.imread('path/to/image')
4

```

```

5 alpha = 1 # contrast
6 beta = 60 # brightness
7 bright_img = cv2.convertScaleAbs(image, alpha=alpha, beta=beta)
8
9 cv2.imwrite('{}{}'.format(newdir_path, filename), bright_img)

```



Figure 5.8: The original image (Figure 5.3) modified by the brightening code. The image appears more washed out, as all colours are move similar due to them having moved closer to white.

5.3 Neural Network

5.3.1 Setting up the Neural Network

Using Python and TensorFlow enabled the authors to exchange the components of the neural network without much effort. This enabled a fast development of a working prove of concept. The structure of the neural network depicted in Figure 5.9 was the first one tested and already proved effective.

In the first test run only 50 greyscale images where used. This encourages overfitting and was only intended to test if the neural network was syntactically set up correctly.

As an optimizer the authors chose stochastic gradient descent as the other optimizers available in TensorFlow are only variations of this optimizer.

5.3.2 Problems Encountered: Normalizing

At this point in time the first problem arose. The accuracy when training the neural network always was equal to one, meaning that the distance to the object in all images was estimated correctly to the last millimetre, which does not seem plausible. Even if the neural network was overfitting, the accuracy should at least in the beginning have a value less than one.

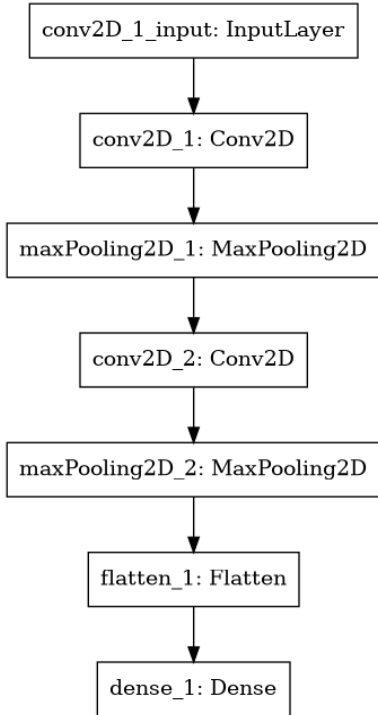


Figure 5.9: A sequential model of a neural network. The input layer receives the greyscale images. The image is then processed by two convolutional layers, each followed by a max pooling layer reducing the width in one dimension and therefore reducing the number of weights. The last layer, a dense layer, outputs the number representing the normalized distance the neural network estimated. The input of this dense layer is a unrolled version of the output of the last max pooling layer. This is achieved by the flatten layer.

It appeared later that this was due to the fact, that the true as well as the estimated output values were not normalized. In a neural network the output of each node has to be between zero and one. As all true values (the distance to the object outputted by Blender) where above one they where simply converted to a value of one. The neural network was trained to only output one, which it easily managed to do, and therefore received an accuracy of one. Normalizing the distances was a simple task as the maximum distance in the generated images was 10 meters. Therefore simply dividing by the maximum possible value reduced the range of the values into the normalized form. This however had the consequence that the accuracy of the neural network was zero, however long it was trained.

5.3.3 Problems Encountered: Accuracy and Metrics

At this point it is noteworthy that in machine learning one can distinguish between classification and regression problems. In classification problems the output value can only be one of a discrete set of values. For example image classification, where a machine learning algorithm labels images as either depicting a cat or a dog. In this example two possible output values

are defined. Regression problems however are identified by the output value being able to take any continuous value. The distance estimation problem described in this thesis is a regression problem, as the distance to the object can be any value between zero and ten. Accuracy is a system of measurement which describes how often the machine learning algorithm “guessed” the correct output. If the output differs in the last decimal place (in our case less than a nano meter) the accuracy does not get increased. Therefore accuracy is only used in classification problems, where the accuracy gets increased for example for correctly guessing that an image depicts a cat (the output matching the actual value exactly). The equivalent used in regression problems is called metric. The metric chosen by the authors is the mean absolute percentage error. It represents a difference between the actual and the output value as a percentage. The lower this percentage the better the performance of the neural network.

5.3.4 Problems Encountered: Number of Training Images

After these modifications the output seemed plausible enough to increase the number of training images from 50 to 10000. Up to this point all images were loaded and converted into tensors before the actual training began. This posed no problem when loading 50 images, however loading 10000 images was not possible with the limited RAM installed on the machine. Since the process was running on a Linux machine, the kernel killed the process due to resource starvation.

The most obvious solution was to split the images into smaller sections and only load and process one of these batches at a time. Additionally the authors chose to store the computed weights after each of these batches, enabling the user to stop the training at any given point in time and still have the relatively new weights stored. When starting the program again, the weights are loaded and training can resume.

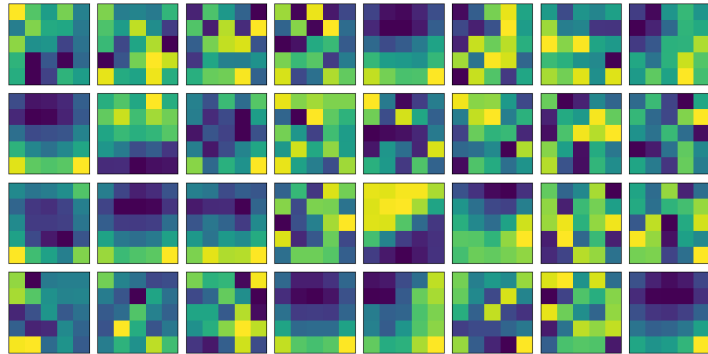
5.3.5 First Results

The first serious training run was performed on 2500 binocular images of a single object. Therefore it was expected, that the neural network would overfit and not work on any other objects. The setup of layers chosen was the one depicted in Fig. 5.9.

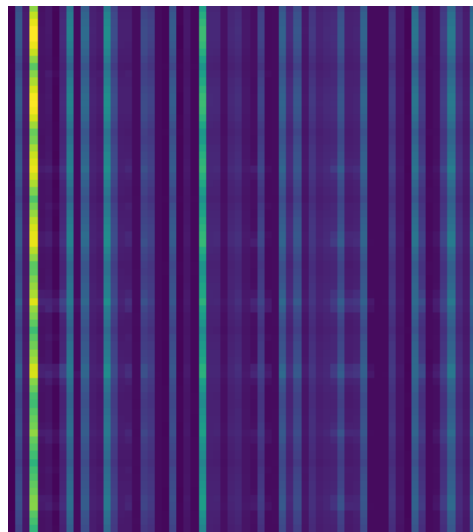
While training the loss sank from around 210,000,000 after having “seen” 50 images to a value of fluctuating between 0.21 and 0.27 while the mean absolute percentage error decreased to a value fluctuating between 11.1% and 16.5%.

The weights of this trained neural network are visualized in Fig. 5.10 and Fig. 5.11. While interpreting weights of a neural network is a vague science, some features of these weights are worth mentioning. For example a few of the matrices shown in Subfig. 5.10a have a dark blue blob appear in the upper middle part, while the bottom left and right pixels show the brightest colours. Since brighter colours mean more influence of the input value received, the authors guess, that the size of objects could be determined by these convolution windows. These convolution windows could for example react to the size of the mount of the object, which is located in the lower part of the image. The second convolutional layer (Subfig. 5.11a) is hard to interpret, as the tensors are already quite abstract at this point. The dense layer (Subfig. 5.10b), however, gives a low weight to most input values, only using some for the

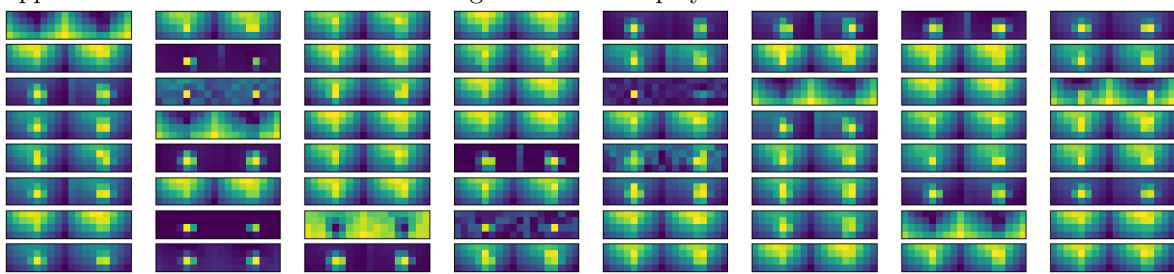
calculation of the final output. Even more interesting are the horizontal stripes appearing in the weights of the dense layer. To get a better understanding of why these stripes appear the authors decided to group the weights of this layer into the sizes of the output of the last convolutional layer. The resulting image can be found in Subfig. 5.10c. From this it is apparent, that the neural network is able to work out that the input image consists of two separate renders. Most of these units focus on the two middle part of the two images separately, some on a larger a region, while other only on the exact place where the object is located. Only few units focus on the section where the shadow of the object is located.



(a) The already trained weights of the first convolutional layer. Each of the 5x5 pixel matrices displays the weights of one layer of the convolution window.

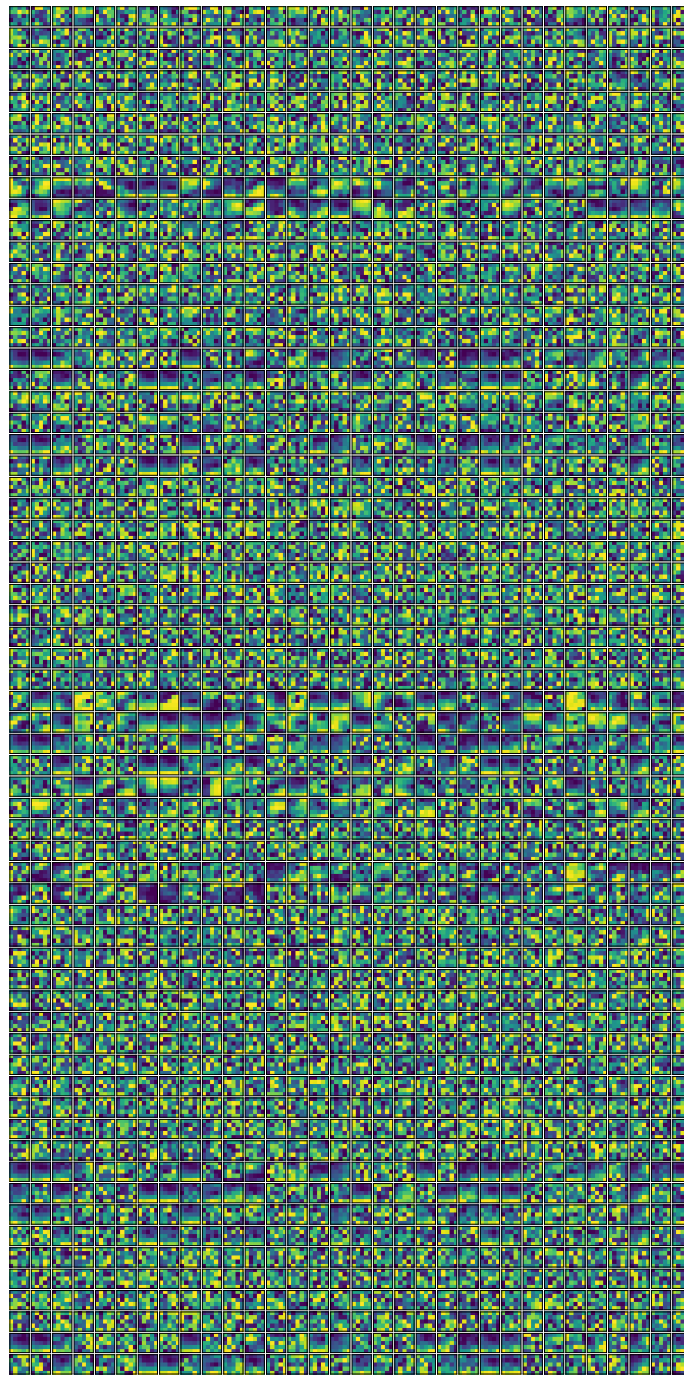


(b) The trained weights of the dense layer, which outputs the estimated result. Horizontal stripes appear because the one dimensional weight vector is displayed as a 72x64 matrix for convenience.



(c) The same weights as in Subfig. 5.10b regrouped into 64 4x18 units.

Figure 5.10: In all subplots the highest value occurring in a unit of pixels is displayed as a yellow colour and the lowest value occurring is a dark blue colour. All other values are shown as the corresponding colours ranging from yellow over green to dark blue.



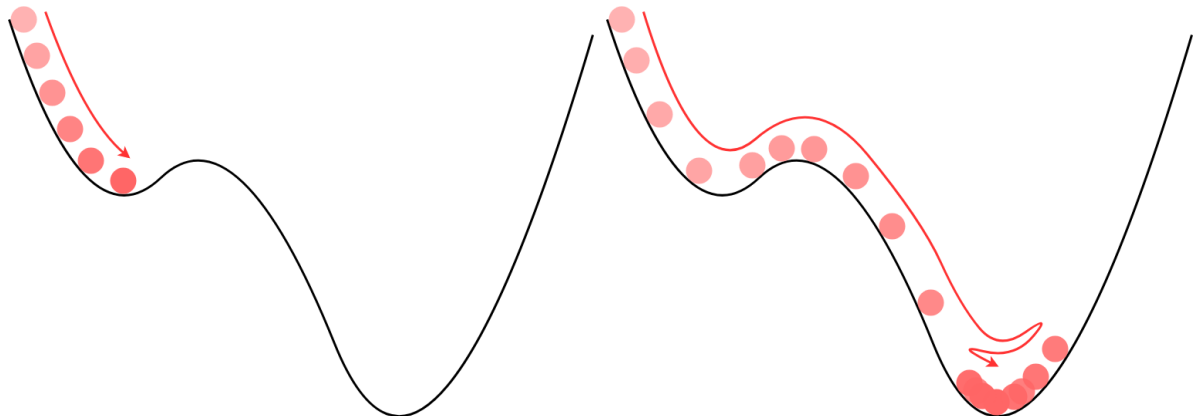
(a) The trained weights of the second convolutional layer. Again each of the 5x5 pixel matrices displays the weights of one units that make up the second convolution window.

Figure 5.11: As in Fig. 5.10 all subplots display the values ranging from yellow (high value) to dark blue (low value).

5.3.6 Modifications to the Neural Network

Since the authors wanted to reach an accuracy of $\pm 10\%$ and the first test only performed with an accuracy of around $\pm 14\%$ possible modifications to the neural network where tested. One of these modifications is the number of epochs, which control how often all images in the input data are used to train the neural network with. E.g. setting the number of epochs to three makes the fit method go through all input images three times. As it turned out increasing the number of epochs does not have any measurable affects on the performance. Therefore the value was set to a count of two epochs.

The next change to the structure of the neural network was the introduction of a momentum term. A momentum term helps to avoid getting stuck in a local, but not the lowest, minimum. One can imagine the optimizer as a mechanism which lets a sphere “roll” down a surface to find the minimum value. A two dimensional version of this is visualized in Fig. 5.12. When no momentum term is defined training behaves as if the sphere had no inertia, which can lead to it getting stuck in a valley, which is not the lowest reachable point. When inertia is added the change in the position of the sphere depends not only on the gradient of the curve in the current position of the sphere, but also on the last few gradients the sphere “rolled” along. Therefore the sphere in Subfig. 5.12b manages to find a lower minimum of the curve.



(a) Visualization of the optimization without a momentum term. The red sphere gets stuck in a local minimum, but fails to find the lowest possible point reachable.
(b) Visualization of the optimization with a momentum term defined. Here the red sphere has enough inertia to “roll” over the small bump, which enables it to reach the lower local minimum.

Figure 5.12: Two figures showing representations of optimization functions. In both cases the optimisation is complete when the red sphere reached a local minimum. The difference in the figures is the use of a momentum term.

In the case of the Neural Network described in the previous sections the addition of a momentum term sadly did not produce better results, as the mean absolute percentage error once again reached a value of around 14% before fluctuating by the same divergence as before. Since the modification of the neural network using a momentum term was not sufficient the authors decided to test whether changing the number and type of layers would change the results. At first one of the convolutional layers was swapped for a dense layer. This led to

a remarkable decrease in the accuracy reached after training on only 500 images. Therefore the authors decided to test if increasing the number of convolutional layers would yield the opposite results. The resulting layer setup of the neural network can be found in Fig. 5.13.

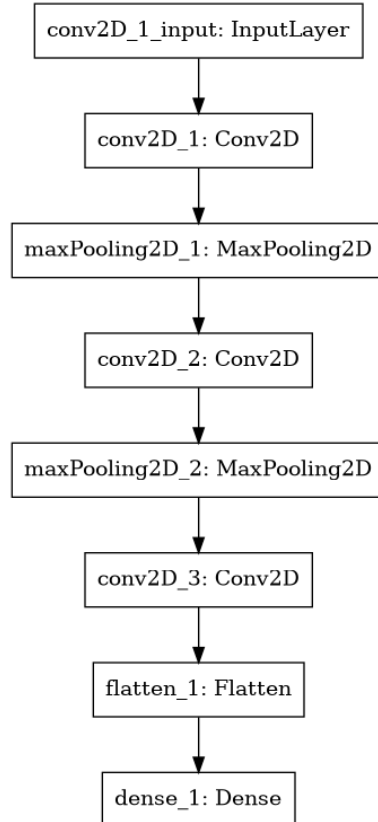


Figure 5.13: The layer structure from Fig. 5.9 modified to include an additional convolutional layer.

With this new setup the neural network was able to recognise the distance to a single object with a 13% accuracy after having seen as little as 300 images of the object. While this still does not reach the desired accuracy, needing fewer images to train the neural network is still an improvement.

5.4 C++ Implementation

The next step for the authors was implementing a neural network in C++ from scratch. This implementation would then be compared to Tensorflow by solving the same task with a neural network. The reason for this comparison is for the authors to see, how much a neural network can be optimized in order to achieve machine learning faster. Therefore the C++ implementation will not be heavily optimized, but rather just usable for any kind of machine learning with neural networks in order to see the difference.

5.4.1 Structure

The C++ implementation consists of three main parts: One major part is the neural network itself. The second part is for measuring time and the third part is for all math, such as some activation functions. Because the second and the third part should be self-explanatory the authors will just focus on the first and also largest part - the neural network.

The Neural Network in C++

The neural network is designed to be a sequence of layers, which consist of several nodes. There are three types of layers:

1. Input Layers
2. Hidden Layers
3. Output Layers

There can only be one input layer and one output layer. The main difference between the three types is that input layers have no connection to them, since they represent the input. Output Layers have no connection from them, because they are the final output. Hidden layers have both connections to and from them. Connections are achieved in the Node class via two lists (in C++ as a std::vector): One list stores all weights and the second list stores the neighbours of the next layer.

So to conclude: A node references the nth neighbour via the nth weight. The connection of layers happens in the NeuralNetwork class with a call to NeuralNetwork::create(). Before this call is made, the layers have to be added with NeuralNetwork::add_layer() first. As parameters this method requires the type of layer, the number of nodes in the layer and the number of connections per node to the next layer's nodes, which is regarded to as the dimension of the layer. If the dimension is one then every node has exactly one neighbour in the next layer (except for nodes in the output layer, of course. In this case the dimension is always 0). If the dimension is the number of nodes in the next layer, we speak of a dense layer, where every node of the added layer is connected to every node of the next layer.

The Application class

With the neural network implementation done the first major part is finished, but we are still missing the learning process. In order to abstract that there exists the Application class. The authors tried to make it as simple and user-friendly as possible, so all needed to train your created neural network is creating an instance of this class, which means calling the constructor. The constructor needs a few things:

1. The reference to the created neural network
2. The inputs for the neural network
3. The expected outputs for the neural network

4. The number of epochs (The number of times it should train)
5. The learning rate it should train with
6. (Optional) A logging stream (can be a filestream or stdout, for example)
7. (Optional) (Bool) More verbose output (increases training time)

The inputs are used to initialize the nodes in the input layer. With help of the hidden layers the goal of the training procedure is to have an output layer holding the values of the outputs. Putting it all together - the following code achieves learning bitwise AND with 10000 epochs and a learning rate of 0.15 in just under 37 milliseconds:

```

1 #include <vector>
2 #include <fstream>
3
4 #include "NeuralNetwork.h"
5 #include "Timer.h"
6
7 int main()
8 {
9     nn::core::NeuralNetwork neural_net;
10    neural_net.add_layer(2, 2, nn::core::LayerType::Input);
11    neural_net.add_layer(2, 1, nn::core::LayerType::Hidden);
12    neural_net.add_layer(1, 1, nn::core::LayerType::Output);
13    neural_net.create();
14
15    // Expected inputs/outputs
16    std::vector<std::vector<float>> input_sets{{1.f, 1.f}, {1.f, 0.f}, {0.f, 1.f},
17        {0.f, 0.f}};
18    std::vector<std::vector<float>> output_sets{{1.f}, {0.f}, {0.f}, {0.f}};
19
20    std::ofstream log{"logfile.log"};
21    nn::benchmark::Timer t{"AND learning"};
22
23    nn::core::Application and_training{neural_net, input_sets, output_sets, 10000,
24        0.15f, log};
25 }
```

5.5 Technical difficulties

Chapter 6

Experiment 1

Author:

6.1 Environment

[TODO: viele Fotos] [TODO: Hintergrundfarbe, Untergrundfarbe, Struktur (Hintergrund und Untergrund), Beleuchtung (Art, Helligkeit, Richtung, mehrere Lichtquellen, welche Lichtquellen, ...)]

6.2 Setup

[TODO: viele Fotos] [TODO: welche Objekte (Größe, Farbe, wie viele (mindestens 3)?, ...), Kameras, Entfernung zu Objekten]

6.3 Sequence of Events

6.4 Results

Chapter 7

Lessons learned

Author:

Chapter 8

Experiment 2

Author:

8.1 Environment

[TODO: viele Fotos]

8.2 Setup

[TODO: viele Fotos]

8.3 Materials

[TODO: viele Fotos]

8.4 Sequence of Events

8.5 Results

Chapter 9

Conclusion

Author:

Index

Authors Index

- Bresenham, Jack, 7
Cormack, Robert, 9
Gibson, Eleanor J, 11
Hagen, Margaret A, 10
K.T. Gribbon C.T. Johnston, Donald G.
Bailey, 5
Mühlmann, Karsten, 7
Open Source Robotics Foundation, Inc.,
27
Richards, Whitman, 9
Rogers, Brian, 10
SAS, Parrot Drones, 3
Scharstein, Daniel, 8
Schrater, Paul R, 9
Sprunk, Christoph, 8
Tom Hope Yehezkel S. Resheff, Itay
Lieder, 23
William F. Ganong, MD, 10
Yonas, Albert, 10
Zezhi Chen Chengke Wu, Hung Tat Tsui,
7

Literature Index

- A linear algorithm for incremental digital display of circular arcs*, 7
A new image rectification algorithm, 7
A real-time FPGA implementation of a barrel distortion correction algorithm with bilinear interpolation, 5
Calculating Dense Disparity Maps from Color Stereo Images, an Efficient Implementation, 7
Convergence as a cue to depth, 9
Development of ability to perceive and produce pictorial depth cue of overlapping, 10
Documentation - roswiki, 27
High-accuracy stereo depth maps using structured light, 8
How optimal depth cue integration depends on the task, 9
Infants' distance perception from linear perspective and texture gradients, 10

Learning TensorFlow, 23
Lidar-based teach-and-repeat of mobile robot trajectories, 8
Motion parallax as an independent cue for depth perception, 10
Parrot Bebop 2 Specifications, 3
Review of Medical Physiology, 10
The computation of retinal disparity., 9
The visual cliff, 11

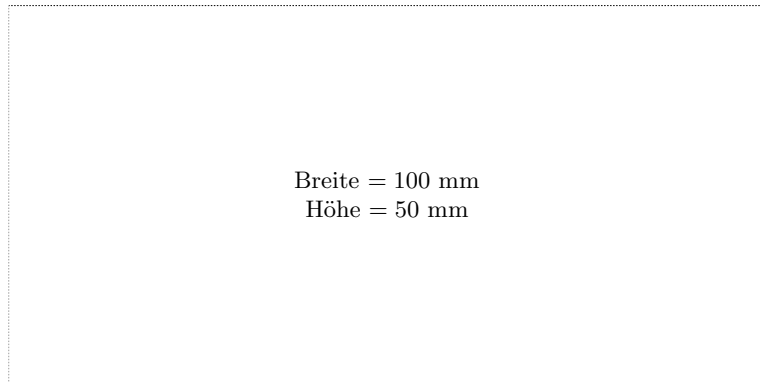
Bibliography

- Bresenham, Jack. “A linear algorithm for incremental digital display of circular arcs”. In: *Communications of the ACM* 20.2 (1977), pp. 100–106.
- Cormack, Robert and Robert Fox. “The computation of retinal disparity.” In: *Perception & Psychophysics* (1985).
- Gibson, Eleanor J and Richard D Walk. “The visual cliff”. In: *Scientific American* 202.4 (1960), pp. 64–71.
- Hagen, Margaret A. “Development of ability to perceive and produce pictorial depth cue of overlapping”. In: *Perceptual and Motor Skills* 42.3 (1976), pp. 1007–1014.
- K.T. Gribbon C.T. Johnston, Donald G. Bailey. “A real-time FPGA implementation of a barrel distortion correction algorithm with bilinear interpolation”. In: *Image and Vision Computing New Zealand*. 2003, pp. 408–413.
- Mühlmann, Karsten, Dennis Maier, Jürgen Hesser, and Reinhard Männer. “Calculating Dense Disparity Maps from Color Stereo Images, an Efficient Implementation”. In: *International Journal of Computer Vision* 47.1 (Apr. 2002), pp. 79–88. ISSN: 1573-1405. DOI: 10.1023/A:1014581421794. URL: <https://doi.org/10.1023/A:1014581421794>.
- Open Source Robotics Foundation, Inc. *Documentation - ros wiki*. 2019. URL: <https://wiki.ros.org>.
- Richards, Whitman and John F Miller. “Convergence as a cue to depth”. In: *Perception & Psychophysics* 5.5 (1969), pp. 317–320.
- Rogers, Brian and Maureen Graham. “Motion parallax as an independent cue for depth perception”. In: *Perception* 8.2 (1979), pp. 125–134.
- SAS, Parrot Drones. *Parrot Bebop 2 Specifications*. 2019. URL: <https://www.parrot.com/us/drones/parrot-bebop-2>.
- Scharstein, Daniel and Richard Szeliski. “High-accuracy stereo depth maps using structured light”. In: *2003 IEEE Computer Society Conference on Computer Vision and Pattern Recognition, 2003. Proceedings*. Vol. 1. IEEE. 2003, pp. I–I.
- Schrater, Paul R and Daniel Kersten. “How optimal depth cue integration depends on the task”. In: *International Journal of Computer Vision* 40.1 (2000), pp. 71–89.
- Sprung, Christoph, Gian Diego Tipaldi, Andrea Cherubini, and Wolfram Burgard. “Lidar-based teach-and-repeat of mobile robot trajectories”. In: *2013 IEEE/RSJ International Conference on Intelligent Robots and Systems*. IEEE. 2013, pp. 3144–3149.
- Tom Hope Yehezkel S. Resheff, Itay Lieder. *Learning TensorFlow*. O'Reilly, 2017.
- William F. Ganong, MD. *Review of Medical Physiology*. Appleton and Lange, 1997.

- Yonas, Albert, Carl E Granrud, Martha E Arterberry, and Brenda L Hanson. "Infants' distance perception from linear perspective and texture gradients". In: *Infant Behavior and Development* 9.3 (1986), pp. 247–256.
- Zezhi Chen Chengke Wu, Hung Tat Tsui. "A new image rectification algorithm". In: *Pattern Recognition Letters* 24.1-3 (2003), pp. 251–260.

Messbox zur Druckkontrolle

— Druckgröße kontrollieren! —



Breite = 100 mm
Höhe = 50 mm

— Diese Seite nach dem Druck entfernen! —